

## Coherent electronic backscattering in ballistic microstructures

M. J. Berry, J. H. Baskey, and R. M. Westervelt

*Division of Applied Sciences and Department of Physics, Harvard University, Cambridge, Massachusetts 02138*

A. C. Gossard

*Materials Department, University of California, Santa Barbara, California 93106*

(Received 6 June 1994)

A magnetoresistance peak at zero magnetic field due to coherent backscattering is studied in submicrometer quantum dots with quantum-point-contact leads. A systematic series of experiments on ballistic microstructures shows that coherent backscattering is distinct from conductance fluctuations at finite fields and gives properties in agreement with semiclassical theory. The effect results from interference between pairs of time-reversed paths of ballistic electrons scattered from the walls of the dot, analogous to weak localization in diffusive systems.

Coherent backscattering is ubiquitous to wave propagation in disordered media, where multiple scattering leads to complicated paths through the medium. The probability to return to the origin is increased by constructive interference between pairs of time-reversed paths. Occurring for both sound<sup>1</sup> and light,<sup>2</sup> coherent backscattering has been studied extensively for electron waves diffusing through a spatially random impurity potential, where it is known as weak localization.<sup>3,4</sup> The predictions of weak-localization theory have been verified through studies of the magnetoresistance peak at zero magnetic field in disordered conductors.<sup>3,4</sup> In ballistic microstructures, coherent backscattering can also occur from interference between pairs of time-reversed electron paths scattering from the walls of the structure, each path starting and ending in the same point-contact mode. A zero-field resistance peak has recently been discovered in circular and stadium-shaped ballistic microstructures and associated with an analog of weak localization.<sup>5</sup> This identification is supported by later theory<sup>6</sup> and subsequent experiment results.<sup>7,8</sup>

In this paper, we demonstrate that coherent backscattering is the cause of the zero-field resistance peak in stadium-shaped ballistic microstructures, and that this effect is distinct from conduction fluctuations at finite fields. The low-temperature ( $T \leq 1.50$  K) magnetoresistance exhibits a prominent zero-field peak and reproducible, aperiodic conductance fluctuations. The zero-field peak is distinguished from conductance fluctuations, because it is robust to changes in the impurity configuration or in the number of modes in the point-contact leads, while the conductance fluctuations rearrange dramatically. A comparison of large and small stadia which are otherwise nominally identical demonstrates that the source of both the zero-field peak and conductance fluctuations is scattering of ballistic electrons from the walls of the microstructure. Theory predicts that the characteristic field required to destroy coherent backscattering is approximately one-half that to change conductance fluctuations.<sup>6</sup> We verify this result experimentally by

comparing the half-width of the zero-field resistance peak to the slope of the conductance fluctuation power spectrum.<sup>5,9</sup>

The experiment was carried out on samples fabricated from a GaAs/Al<sub>0.3</sub>Ga<sub>0.7</sub>As heterostructure containing a near-surface two-dimensional electron gas located 420 Å below the surface. The measured sheet density  $n_s = 4.4 \times 10^{11} \text{ cm}^{-2}$  and mobility  $\mu = 350\,000 \text{ cm}^2/\text{V sec}$ , give a transport mean free path  $l = 3.8 \text{ } \mu\text{m}$ . A stadium-shaped quantum dot with quantum point contacts is defined by depleting the electrons under a single metallic gate with a negative voltage bias. Two small stadia and two large stadia were patterned side-by-side on the same chip using electron-beam lithography and Cr/Au metallization. Electron micrographs of a large and a small stadium are shown in Figs. 1(a) and 1(b). They have nominally the same shape and point-contact geometry, differing only in their size. The large stadium [Fig. 1(a)] has dimensions  $18 \times 38 \text{ } \mu\text{m}^2$ , roughly  $7l$ . The small stadium [Fig. 1(b)] has dimensions  $0.62 \times 1.3 \text{ } \mu\text{m}^2$ , roughly  $l/4$ , but much larger than the Fermi wavelength  $\lambda_f = (2\pi/n_s)^{1/2} = 38 \text{ nm}$ , so that the semiclassical picture is appropriate. The point contacts for both stadia have a lithographic width  $\approx 190 \text{ nm}$ , and accommodate up to seven transverse modes when the stadium is defined. The area of the small stadium, estimated as the lithographic area minus a gate voltage-dependent depletion width, decreases from  $0.62$  to  $0.47 \text{ } \mu\text{m}^2$  as the number of modes in the leads decreases from seven to one. The estimated area agrees with the area  $0.48 \text{ } \mu\text{m}^2$  measured by Aharonov-Bohm oscillations with one mode in each lead.

We use the term ballistic to mean that the transport mean free path is larger than the dimensions of the stadium. However, the ballistic regime is not free from disorder: electron trajectories deviate from straight lines within the small stadium because of small-angle scattering,<sup>10</sup> and they scatter from the walls at nonspecular angles because of boundary roughness.<sup>11</sup> Disorder can change regular electron trajectories in highly symmetric structures such as a circular dot into chaotic trajectories,

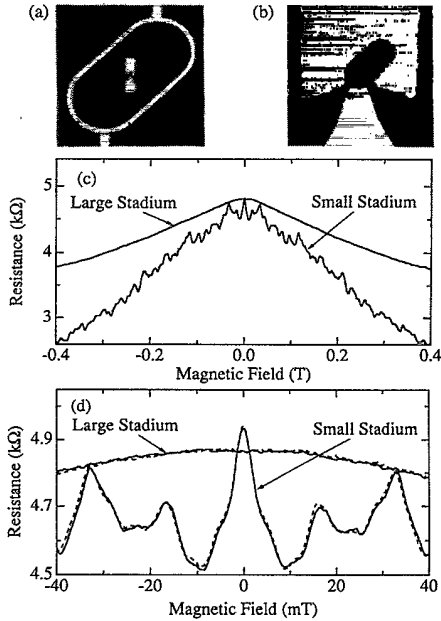


FIG. 1. Electron micrographs of the (a) large and (b) small stadia. (c) Magnetoresistance at  $T=1.50$  K for large and small stadia. Data are taken from a large stadium that does not have a small stadium inside it. (d) Pairs of consecutive traces plotted on an expanded scale demonstrate reproducibility.

but should have less qualitative effect in stadium-shaped structures where the electron trajectories are already highly chaotic.<sup>12</sup> Note that small-angle scattering alone is not sufficient to produce coherent backscattering in quantum dots with dimensions less than the transport mean free path.

The samples were cooled in a  $^3\text{He}$  cryostat or He dilution refrigerator, and magnetoresistance measurements were made using standard ac lock-in techniques. The magnetic field  $B$  is oriented perpendicular to the plane of the electron gas, and the precision of the magnetic-field sweeps was  $\pm 0.01$  mT. We current bias at  $f=11$  Hz using an excitation of  $I_{\text{bias}}R_{\text{sample}} < 0.5$  kT/e. Larger bias currents did not alter the magnetoresistance for  $I_{\text{bias}}R_{\text{sample}} < 5$  kT/e.

Figures 1(c) and 1(d) compare the magnetoresistance of the large and small stadia measured at  $T=1.50$  K.<sup>13</sup> The data are symmetric in magnetic field  $R(B) \approx R(-B)$  as expected for two-probe measurements,<sup>4</sup> with small deviations arising in the wide regions of the electron gas used to make contact. This two-probe symmetry is crucial, because it implies that the magnetoresistance originates in the cavity and not the leads. As shown in Fig. 1(c), the magnetoresistance for the large stadium decreases smoothly from zero field, while the magnetoresistance for small stadium shows a narrow zero-field peak and aperiodic conductance fluctuations superimposed on this smooth background. Figure 1(d) shows an expanded view of two consecutive magnetoresistance sweeps for each stadium. The slight variations from the smooth background seen in the large stadium do not reproduce, while the features in the small stadium accurately reproduce and are clearly well above the noise.

The primary difference between the large and small

stadia responsible for the appearance of the zero-field peak and conductance fluctuations is that both the transport mean free path and the phase-coherence length are smaller than the large stadium, but larger than the small stadium. Thus the large stadium acts as a region of two-dimensional electron gas with quantum point contacts, while the small stadium is a ballistic quantum dot. The phase-coherence time  $\tau_\phi$  was measured on a narrow channel<sup>14</sup> from an adjacent piece of the same wafer, using the method of Ref. 15. The measured value at  $T=1.50$  K is  $\tau_\phi \approx 33$  ps, which gives a ballistic phase-breaking length  $l_\phi \equiv v_F \tau_\phi \approx 9.5$   $\mu\text{m}$ . In order to produce quantum interference, the total path length must be less than  $l_\phi$ . In the small stadium, this length corresponds to roughly ten bounces off the walls, but in the large stadium electrons cannot travel once across before losing their phase. Thus the zero-field peak and conductance fluctuations present in the small stadium are due to quantum interference.

The lack of a resistance peak and conductance fluctuations in the large stadium imply that phenomena seen in the small stadium are due to collisions with the walls of the microstructure. If the zero-field resistance peak in the small stadium were caused by scattering from impurities within the stadium, a similar peak should also be seen in the large stadium. Furthermore, the half-width at half-maximum  $B_c \approx 3$  mT of the zero-field peak for the small stadium is comparable to the field necessary to destroy coherent backscattering in a ballistic quantum dot (see below for a precise comparison), but is a factor  $\sim 150$  larger than the characteristic field  $B_{c,2D} \approx 0.02$  mT necessary to destroy traditional weak localization in a diffusive two-dimensional electron gas with the same scattering times.<sup>3</sup> Note that these arguments are valid for both smooth and rough boundaries, and thus we cannot determine the importance of boundary roughness from this comparison alone.

Figures 2(a) and 2(b) show data which demonstrate

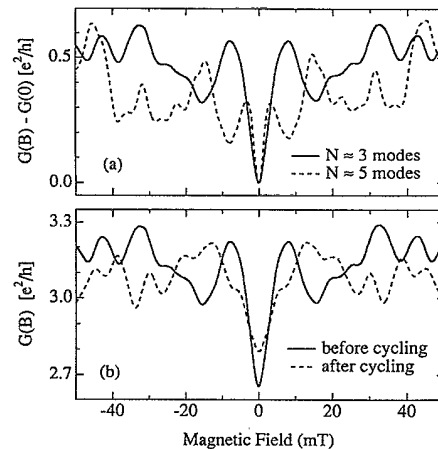


FIG. 2. (a) Conductance change  $G(B)-G(0)$  at  $T=1.50$  K for small stadium with three (solid) and five (dashed) modes in the contacts. (b) Magnetoconductance with three modes before (solid) and after (dashed) thermal cycling.

that the physical origins of the zero-field resistance peak and conductance fluctuations are different. Conductance fluctuations, which can either increase or decrease the conductance, exist at zero field along with coherent backscattering, which only decreases the conductance. Because conductance fluctuations are quite sensitive to small changes in electron trajectories, coherent backscattering can be distinguished by making small changes in the shape of the stadium. In Fig. 2(a), the magnetoconductance of the small stadium is shown for two gate voltages corresponding to approximately three and five modes in each point-contact lead; the magnetoresistance peak here appears as a conductance dip. As shown, the zero-field dip remains prominent, but there is no consistent relationship between the conductance fluctuations in the two cases. Similarly, in Fig. 2(b), the magnetoconductance of the small stadium with three modes in each lead is compared before and after thermal cycling, which rearranges the random potential due to charged impurities. Again, the zero-field dip remains strong, while the conductance fluctuations change dramatically.

Coherent backscattering theory<sup>6</sup> predicts that the zero-field conductance dip is destroyed when one flux quantum threads twice the characteristic area enclosed by paths returning to the injecting contact. By contrast, conductance fluctuation theory<sup>9</sup> predicts that conductance fluctuations will change when one flux quantum is inserted into the characteristic area enclosed by two trajectories joining the injecting and receiving contacts. If one assumes that these two areas are the same, then the characteristic fields  $B_c$  for coherent backscattering and  $B_\alpha$  for conductance fluctuations, defined below, differ by a factor of 2:  $B_c = B_\alpha/2$ ; however, this relationship is not rigorous. Both characteristic fields can be measured from a single magnetoresistance trace in order to test theory.

Figure 3(a) shows representative raw magnetoconductance data from the small stadium at  $T=1.50$  K. The

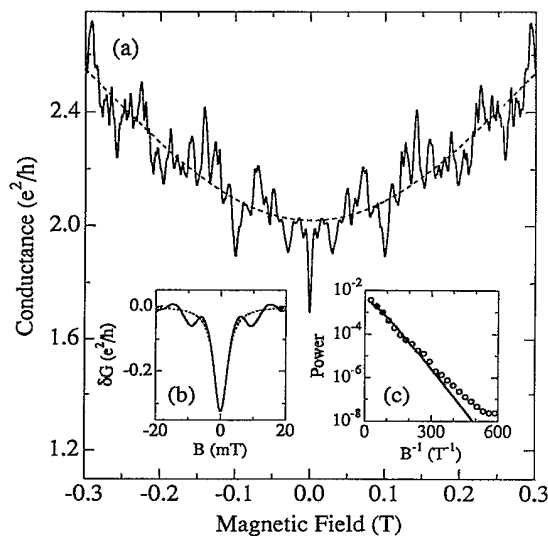


FIG. 3. (a) Magnetoconductance at  $T=1.50$  K (solid) shown with a fourth-order polynomial background fit (dashed). (b) Zero-field conductance dip (solid) with a Lorentzian fit (dashed). (c) Averaged power spectrum of conductance fluctuations (circles) with a fit (solid) to semiclassical theory.

data are only shown at relatively low magnetic fields for which the cyclotron radius is greater than the radius of curvature of the stadium. In order to characterize the zero-field dip and the conductance fluctuations, the slow magnetoconductance background is removed by subtracting a fourth-order polynomial (dashed line) to obtain the difference  $\delta G$ . Baranger, Jalabert, and Stone<sup>6</sup> predict that the zero-field magnetoconductance dip is a Lorentzian. Figure 3(b) shows a fit of a Lorentzian to the data using one free parameter: the half-width at half-maximum  $B_c = 2.5 \pm 0.4$  mT; the height of the dip  $\Delta G_0$  is determined by the background fit. Jalabert, Baranger, and Stone<sup>9</sup> predict that the power spectrum of the conductance fluctuations has a nearly exponential form:  $S(f) = S_0(1 + 2\pi f B_\alpha) \exp(-2\pi f B_\alpha)$ , where  $f$  is expressed in cycles/T. The measured power spectrum of  $\delta G$  versus  $1/B$ , shown as open circles in Fig. 3(c), is obtained by averaging 31 half-overlapping power spectra segments to suppress sharp structure at low frequencies associated with periodic orbits. A fit of  $S(f)$  to the data using two parameters  $B_\alpha$  and  $S_0$ , shown as the solid line in Fig. 3(c), fits well over four orders of magnitude, and gives the characteristic field  $B_\alpha = 5.0 \pm 1.0$  mT.<sup>16</sup> We find  $B_c = B_\alpha/2$  within the error bars, as predicted by semiclassical theory.

Figure 4 shows the dependence of the fluctuating part of the magnetoconductance  $\delta G$  at  $T=1.50$  K as the number of transverse modes in the quantum point contacts increases from  $\approx 1$  in Fig. 4(a) to  $\approx 6$  in Fig. 4(e). A prominent zero-field conductance dip is seen in all five traces, while the conductance fluctuations change. Several trends are evident. The size of the zero-field dip  $\Delta G_0$  increases with the number of modes in the leads, while the width  $B_c$  remains approximately constant. The average root-mean-squared fluctuation  $\delta G_{\text{rms}}$  increases with the number of modes like  $\Delta G_0$ , while fits of  $S(f)$  to the power spectrum of each trace show that the characteristic field  $B_\alpha$  remains approximately constant like  $B_c$ . The fact that  $B_c$  and  $B_\alpha$  are unaffected by changes in the contact width indicate that the characteristics areas at 1.5 K are limited primarily by dephasing inside the dot.<sup>17</sup>

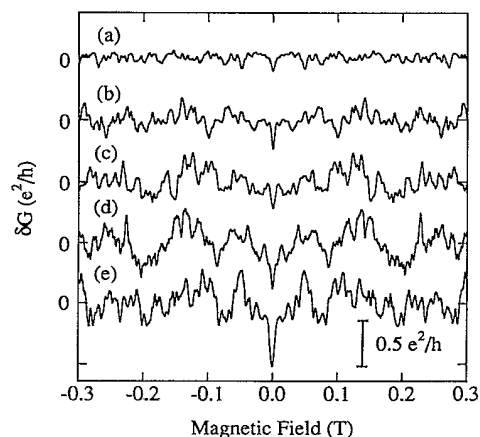


FIG. 4. Conductance change  $\delta G$  at  $T=1.50$  K for five different values of the average conductance at zero field; (a) 1.1, (b) 2.0, (c) 3.1, (d) 4.6, and (e)  $6.3 e^2/h$ .

It also indicates that we are justified in averaging the different values of  $B_c$  and  $B_\alpha$ . The measured statistical properties of the conductance fluctuations characterized by  $\delta G_{\text{rms}}$  and  $B_\alpha$  are unchanged by thermal cycling to within their error bars.

In order to find ensemble average values of the characteristic fields  $B_c$  and  $B_\alpha$ , we repeated the characterization described in Fig. 3 above at 26 gate voltage values for two thermal cycles and for two separate samples, giving  $\langle B_c \rangle = 3.2 \pm 0.8$  mT and  $\langle B_\alpha/2 \rangle = 2.6 \pm 0.6$  mT. The values agree to within their error bars. Ensemble averaging is necessary to extract the best quantitative estimate of the characteristic field  $B_c$ , because zero-field conductance fluctuations superimposed upon coherent backscattering introduce some error. At lower temperature  $T = 0.15$  K, the characteristic field  $B_\alpha$  for conductance fluctuations decreases to  $\langle B_\alpha/2 \rangle = 1.6 \pm 0.4$  mT, indicating that the characteristic area increases; this value re-

peated after thermal cycling, and agrees with that obtained earlier on a separate, nominally identical stadium  $B_\alpha/2 = 1.8$  mT.<sup>5</sup> A larger area is expected for the longer phase-coherence time  $\tau_\phi$  at lower temperatures. The relative size of the conductance fluctuations increases at low temperatures and makes a detailed analysis of the zero-field conductance dip difficult.

We thank S. H. Yang, J. A. Katine, D. J. Mar, C. M. Marcus, M. W. Keller, and H. U. Baranger for discussions, and P. F. Hopkins for help in sample fabrication. Work at Harvard was supported by Grant Nos. N00014-89-J-1592 and DMR-91-19386, and at UCSB by AFOSR 91-0214. One of us (M.J.B.) acknowledges financial support from the NSF, and one (R.M.W.) acknowledges support from the Center for Quantized Electronic Structures and the Institute for Theoretical Physics at UCSB.

<sup>1</sup>G. Bayer and T. Niederdränk, Phys. Rev. Lett. **70**, 3884 (1993).

<sup>2</sup>M. P. van Albada and A. Lagendijk, Phys. Rev. Lett. **55**, 2692 (1985); P. E. Wolf and G. Maret, *ibid.* **55**, 2696 (1985).

<sup>3</sup>S. Chakravarty and A. Schmid, Phys. Rep. **140**, 193 (1986); G. Bergmann, *ibid.* **107**, 1 (1984), and references therein.

<sup>4</sup>C. W. J. Beenakker and H. van Houten, in *Solid State Physics*, edited by H. Ehrenreich and D. Turnbull (Academic, San Diego, 1991), Vol. 94, and references therein.

<sup>5</sup>C. M. Marcus, A. J. Rimberg, R. M. Westervelt, P. F. Hopkins, and A. C. Gossard, Phys. Rev. Lett. **69**, 506 (1992).

<sup>6</sup>H. U. Baranger, R. A. Jalabert, and A. D. Stone, Phys. Rev. Lett. **70**, 3876 (1993).

<sup>7</sup>M. J. Berry, J. A. Katine, C. M. Marcus, R. M. Westervelt, and A. C. Gossard, Surf. Sci. **305**, 495 (1994).

<sup>8</sup>M. W. Keller, O. Millo, A. Mittal, D. E. Prober, and R. N. Sacks, Surf. Sci. **305**, 501 (1994).

<sup>9</sup>R. A. Jalabert, H. U. Baranger, and A. D. Stone, Phys. Rev.

Lett. **65**, 2442 (1990).

<sup>10</sup>The small angle scattering time measured on the same wafer via Shubnikov-de Haas oscillations (Ref. 14) is  $\tau_s \approx 1.0$  ps.

<sup>11</sup>W. A. Lin, J. B. Delos, and R. V. Jensen, Chaos **3**, 655 (1993).

<sup>12</sup>G. Benettin and J.-M. Strelcyn, Phys. Rev. A **17**, 773 (1978).

<sup>13</sup>Both stadia were biased with approximately the same zero-field conductance corresponding to five transverse modes ( $G \approx 10 e^2/h$ ) in each contact.

<sup>14</sup>M. J. Berry, J. A. Katine, R. M. Westervelt, and A. C. Gossard (unpublished).

<sup>15</sup>H. van Houten, C. W. J. Beenakker, B. J. van Wees, and J. E. Mooij, Surf. Sci. **196**, 144 (1988); C. W. J. Beenakker and H. van Houten, Phys. Rev. B **38**, 3232 (1988).

<sup>16</sup>The error ( $\approx 25\%$ ) is dominated by uncertainty in the fit range.

<sup>17</sup>C. M. Marcus, R. M. Westervelt, P. F. Hopkins, and A. C. Gossard, Phys. Rev. B **48**, 2460 (1993).